J Physiol 588.15 (2010) pp 2823–2838

The Journal of Physiology

Development of calcium-permeable AMPA receptors and their correlation with NMDA receptors in fast-spiking interneurons of rat prefrontal cortex

Huai-Xing Wang and Wen-Jun Gao

Department of Neurobiology and Anatomy, Drexel University College of Medicine, Philadelphia, PA 19129, USA

Abnormal influx of Ca^{2+} is thought to contribute to the neuronal injury associated with a number of brain disorders, and Ca^{2+}-permeable AMPA receptors (CP-AMPARs) play a critical role in the pathological process. Despite the apparent vulnerability of fast-spiking (FS) interneurons in neurological disorders, little is known about the CP-AMPARs expressed by functionally identified FS interneurons in the developing prefrontal cortex (PFC). We investigated the development of inwardly rectifying AMPA receptor-mediated currents and their correlation with NMDA receptor-mediated currents in FS interneurons in the rat PFC. We found that 78% of the FS interneurons expressed a low rectification index, presumably Ca^{2+}-permeable AMPARs, with only 22% exhibiting AMPARs with a high rectification index, probably Ca^{2+} impermeable (CI). FS interneurons with CP-AMPARs exhibited properties distinct from those expressing CI-AMPARs, although both displayed similar morphologies, passive membrane properties and AMPA currents at resting membrane potentials. The AMPA receptors also exhibited dramatic changes during cortical development with significantly more FS interneurons with CP-AMPARs and a clearly decreased rectification index during adolescence. In addition, FS interneurons with CP-AMPARs exhibited few or no NMDA currents, distinct frequency-dependent synaptic facilitation, and protracted maturation in short-term plasticity. These data suggest that CP-AMPARs in FS interneurons may play a critical role in neuronal integration and that their characteristic properties may make these cells particularly vulnerable to disruptive influences in the PFC, thus contributing to the onset of many psychiatric disorders.

(Received 20 January 2010; accepted after revision 10 June 2010; first published online 14 June 2010)
Corresponding author W.-J. Gao: Department of Neurobiology and Anatomy, Drexel University College of Medicine, 2900 Queen Lane, Philadelphia, PA 19129, USA. Email: wgao@drexelmed.edu

Abbreviations AMPA, α-amino-3-hydroxy-5-methyl-4-isoxazolepropionic acid; AP, action potential; CI-AMPARs, Ca^{2+}-impermeable AMPA receptors; CP-AMPARs, Ca^{2+}-permeable AMPA receptors; D-APV, D-(−)-2-amino-5-phosphonopentanoic acid; EPSCs, excitatory postsynaptic currents; FS, fast-spiking; GABA, γ-aminobutyric acid; GluR2, glutamate receptor 2; *I–V*, current–voltage; mEPSCs, miniature EPSCs; NMDA, *N*-methyl-D-aspartic acid; PD, postnatal day; PFC, prefrontal cortex; PPD, paired-pulse depression; PPF, paired-pulse facilitation; PPR, paired-pulse ratio; RI, rectification index.

Introduction

Synaptic transmissions mediated by α-amino-3-hydroxy-5-methyl-4-isoxazolepropionic acid (AMPA) and *N*-methyl-D-aspartic acid (NMDA) receptors in the cortical interneurons control the feedforward and feedback inhibition in the cortical circuitry (McBain & Fisahn, 2001; Maccaferri & Dingledine, 2002; Jonas *et al.* 2004). Many studies in the hippocampus indicated that γ-aminobutyric acid (GABA)-ergic interneurons generally exhibit a significant proportion of glutamate receptor 2 (GluR2)-lacking AMPA receptors (McBain & Dingledine, 1993; Geiger *et al.* 1995; Koh *et al.* 1995; Toth & McBain, 1998, 2000; Isaac *et al.* 2007). The Ca^{2+} permeability of AMPARs is critically dependent on GluR2; those containing GluR2 are Ca^{2+} impermeable (CI-AMPARs) and have a linear current–voltage (*I–V*) relation, and those lacking GluR2 are Ca^{2+} permeable (CP-AMPARs) and strongly inwardly rectifying (Hollmann & Heinemann, 1994; Jonas & Burnashev, 1995). GluR2-lacking CP-AMPARs have recently received considerable attention because of their postulated role in synaptic plasticity (Liu & Cull-Candy, 2000; Clem & Barth, 2006; Plant *et al.* 2006; Adesnik

© 2010 The Authors. Journal compilation © 2010 The Physiological Society
DOI: 10.1113/jphysiol.2010.187591

Downloaded from J Physiol (jp.physoc.org) at Hahneman Univ on August 6, 2010

& Nicoll, 2007) and neurological disorders (Tanaka *et al.* 2000; Cull-Candy *et al.* 2006; Liu *et al.* 2006; Isaac *et al.* 2007; Liu & Zukin, 2007). Although a previous study reported that fast-spiking (FS) interneurons in the rat motor cortex had a relatively small NMDA contribution (Angulo *et al.* 1999*a*), the AMPA and NMDA subtypes expressed by functionally identified neocortical interneurons remained limited (Blatow *et al.* 2005), particulary in the prefrontal cortex (PFC). Recent studies indicated that Ca^{2+} influx in the dendrites of neocortical interneurons is mainly through CP-AMPARs (Goldberg *et al.* 2003) and that pyramidal neurons in the somatosensory cortex lost CP-AMPARs before postnatal day (PD)16 (Kumar *et al.* 2002). In addition, we recently found that FS interneurons in the rat PFC exhibited distinct properties of NMDA currents, particularly during the adolescent period. In juvenile animals (PD15 − 28), most (73%) of the FS cells demonstrated both AMPA and NMDA currents; in adults (∼PD90), only ∼26% contained detectable NMDA currents (Wang & Gao, 2009). Because functional maturation of the PFC is presumably delayed and the underlying synaptic refinement process is usually not completed until late adolescence and early adulthood (Woo *et al.* 1997; Tseng & O'Donnell, 2007; Wang *et al.* 2008), it would be intriguing to identify the functional change that occurs in CP-AMPARs in the developing FS interneurons in PFC. We proposed that FS interneurons in the PFC may use CP-AMPARs for Ca^{2+} influx to compensate for the apparent lack of synaptic NMDA receptors. We tested this possibility by examining the rectification index (RI) of AMPAR-mediated currents in the FS interneurons at different developmental stages. We found that the AMPARs in FS interneurons with many NMDA receptors in the rat PFC displayed a clearly linear *I–V* relationship and paired-pulse depression. In contrast, the AMPARs in FS interneurons with no or few NMDA receptors expressed CP-AMPARs, which exhibited a significantly non-linear *I–V* relationship, prominent synaptic facilitation, and distinct frequency-dependent short-term plasticity. The AMPA receptors also exhibited a significantly decreased RI during adolescence.

Methods

Brain slice preparation and physiological recording

Seventy-three Sprague–Dawley rats of either gender, aged PD15–115, were used in this study. The rats were divided into juvenile (PD15−28), adolescent (PD31−63) and adult (PD86−115) groups as previously reported (Spear, 2000; Tseng & O'Donnell, 2007; Wang & Gao, 2009). The rats were cared for according to National Institutes of Health guidelines, and the experimental protocol was approved by the Institutional Animal Care and Use Committee at Drexel University College of Medicine. The experiments also complied with the policies and regulations of ethical matters in *The Journal of Physiology* (Drummond, 2009). The detailed procedure can be found in our previous studies (Gao & Goldman-Rakic, 2003; Gao *et al.* 2003; Gao, 2007; Wang & Gao, 2009). The rats were deeply anaesthetized with Euthasol (0.2 ml kg^{-1}, I.P.), rapidly perfused with ice-cold (< 4°C) sucrose solution containing (in mM): KCl 2.5, NaH_2PO_4 1.25, $NaHCO_3$ 26, $CaCl_2$ 0.5, $MgSO_4$ 7.0, and sucrose 213, and aerated with 95% O_2 and 5% CO_2. The rats were decapitated with a guillotine; the brains were quickly removed and placed in the same sucrose solution. Horizontal brain slices at 300 μm were made with a Vibratome (Vibratome Co., St Louis, MO, USA), and the slices were incubated in an oxygenated sucrose solution at 35°C for 1 h. The slices were incubated at room temperature until being transferred into a submerged recording chamber. The recordings were conducted with cortical slices perfused with Ringer solution containing the following ingredients (in mM): NaCl 128, KCl 2.5, NaH_2PO_4 1.25, $CaCl_2$ 2, $MgSO_4$ 1, $NaHCO_3$ 26, and dextrose 10, pH 7.4. Whole-cell patch clamp recordings were conducted in the PFC slices through an upright microscope (Olympus BX61, Olympus Optics, Japan) equipped with infrared differential interference contrast optics (IR-DIC). The recordings were conducted at ∼36°C. Resistance of the recording pipette (1.2 mm borosilicate glass) was ∼9 MΩ. Tips of the recording pipettes were first filled with a potassium gluconate-based intracellular solution (∼1 mm from the tip) and then backfilled with a Cs^+-containing solution. The potassium gluconate solution contained (in mM): potassium gluconate 120, KCl 6, ATP-Mg 4, Na_2GTP 0.3, EGTA 0.1, Hepes 10, and 0.3% biocytin, pH 7.3, 310 mosmol L^{-1}; the Cs^+ solution contained (in mM): caesium gluconate 120, QX-314 chloride 5, $CsCl_2$ 6, ATP-Mg 1, Na_2GTP 0.2, Hepes 10, spermine 0.05, and 0.3% biocytin at pH 7.3 (adjusted with CsOH). With this strategy, we were able to record the action potentials immediately (usually within 1 min) after forming a giga-seal due to the presence of a K^+ internal solution at the tip of the patch pipette. Then we could record AMPAR- and NMDAR-mediated currents with minimal K^+ current contamination due to the delayed diffusion (∼5 min) of Cs^+ ions into the recorded cell (Wang & Gao, 2009). The excitatory postsynaptic currents (EPSCs) were evoked by a bipolar electrode placed about 300 μm away from the recorded neurons (0.1 ms, 40–400 μA, 0.1 Hz) in the presence of the $GABA_A$ antagonist picrotoxin (50 μM, Sigma-Aldrich, St Louis, MO, USA). The AMPA receptor-mediated AMPA EPSCs were recorded at −60 mV for the paired-pulse stimulation, whereas the inwardly rectifying AMPA EPSCs were recorded at −60, 0 and +60 mV to calculate the RI (see 'Data analysis') in the presence of picrotoxin and NMDA receptor

© 2010 The Authors. Journal compilation © 2010 The Physiological Society

Downloaded from J Physiol (jp.physoc.org) at Hahneman Univ on August 6, 2010

antagonist D-(−)-2-amino-5-phosphonopentanoic acid (D-APV, 50 μM, Sigma-Aldrich). The *I–V* relationships of AMPA EPSCs were recorded 10 min after break-in to allow sufficient time for diffusion of spermine, and measurements were made from the averages of 15 responses evoked by intracortical stimulation with membrane potentials held at 20 mV steps from −80 mV to +80 mV. The NMDA receptor-mediated currents (NMDA EPSCs) were recorded at +60 mV under conditions of bath-applied picrotoxin and the AMPA receptor antagonist 2,3-dihydroxy-6-nitro-7-sulfamoyl-benzo[f]quinoxaline-2,3-dione (NBQX) (20 μM, Sigma-Aldrich). NMDA EPSCs were confirmed by bath application of D-APV (50 μM) in some cases. To record NMDA receptor-mediated miniature EPSCs (mEPSCs), membrane potentials of FS interneurons were held either at −60 mV in Mg^{2+}-free external solution with bath perfusion of the sodium channel blocker tetrodotoxin (TTX, 0.5 μM) and picrotoxin (100 μM), as described previously (Myme *et al.* 2003) or at +60 mV in the presence of picrotoxin, NBQX and TTX. The access resistance ranged from 18 to 30 MΩ, and the series resistances were constantly monitored through a test hyperpolarizing pulse (5 mV, 200 ms) applied in each sweep and were compensated at regular intervals throughout the recordings. The electric signals were recorded using MultiClamp 700B (Molecular Devices) and acquired at sampling intervals of 20–50 μs through pCLAMP 9.2 software (Molecular Devices).

Histological and morphological analyses

All slices with recorded neurons were preserved for biocytin immunostaining as previously reported (Gao *et al.* 2003; Gao, 2007; Wang & Gao, 2009). Briefly, slices were fixed with 4% paraformaldehyde for at least 24 h; the slices were placed in 3% H_2O_2 for 30 min to block the endogenous horseradish peroxidase. After thorough rinsing, reactions of an avidin/biotinylated enzyme complex (Vector Laboratories, USA) were conducted overnight, followed by the Ni-3,3-diaminobenzidine reaction. The slices were rinsed with 0.1 mM phosphate buffer (pH 7.4), mounted on glass slides, and covered with water-soluble mounting media. All labelled neurons were double-checked to determine that their documented locations and firing patterns matched, for cell type identification.

Data analysis

The action potentials recorded in current clamp mode in the first minute after membrane break-in were used to measure the resting membrane potential, input resistance, action potential (AP) threshold, AP half-width, and after-hyperpolarization. All of these parameters were used to distinguish FS interneurons from other cell types. Detailed procedures can be found in our recent report (Wang & Gao, 2009). Data were rejected for further analysis if the series resistance changed more than 20% during recordings. The amplitudes of the EPSCs were measured by averaging 30 sweeps from the onset to the peak of the EPSCs with Clampfit 9.2 software (Molecular Devices). Only the neurons that produced stable EPSCs for at least 5 min without rundown were used for further analysis. The time constant decay was obtained by fitting the recovery phase of the evoked EPSC with a single exponential function (standard exponential formula) in Clampfit 9.2. The RI for individual FS interneurons was calculated as the amplitude of AMPA-$EPSC_{+60\ mV}$/AMPA-$EPSC_{-60\ mV}$. The reversal potentials were empirically determined by a plot in which zero current crossed the *x*-axis (potential). The paired-pulse ratio (PPR) was determined as the peak amplitude of AMPA EPSC2/EPSC1 in 20 Hz recordings. The mEPSCs recorded in the voltage-clamp mode were analysed with Clampfit 9.2. A typical mEPSC was selected to create a sample template for event detection within a data period, and the AMPA or NMDA mEPSCs were detected with a threshold set at 3 times the value of the root mean square of the baseline noise. For the mEPSCs recorded at −60 mV in zero Mg^{2+} solution, the peak of an mEPSC was taken as the AMPA amplitude, whereas the NMDA current was measured 5 ms after the mEPSC peak. We chose 5 ms instead of the 18–23 ms used for pyramidal cells by Myme *et al.* (see Myme *et al.* 2003) because the decay of AMPA EPSC on the fast-spiking interneurons was usually < 5 ms (Hestrin, 1993; McBain & Dingledine, 1993; Angulo *et al.* 1997; Wang & Gao, 2009), whereas the EPSC decay on pyramidal neurons was ≥15 ms (Hestrin, 1993; McBain & Dingledine, 1993; Myme *et al.* 2003). The NMDA/AMPA ratio for mEPSCs was given as the ratio of these two currents. For the NMDA mEPSCs recorded at +60 mV, the mEPSC amplitude, frequency and 63% decay were directly measured from the averaged mEPSCs. All data were presented as mean ± standard error of the mean along with Student's *t* test, ANOVA, χ^2 test, or Pearson rank correlations to examine the statistical significance.

Results

FS interneurons in the rat PFC can be divided into two distinct subtypes based on the RI in AMPA-mediated EPSCs

Despite the heterogeneous nature of GABAergic interneurons in the neocortex, they are divided physiologically into FS cells and several non-FS cell types (Kawaguchi, 1995; Cauli *et al.* 1997; Xiang *et al.* 1998; Gibson *et al.* 1999; Gao *et al.* 2003). To study the development of AMPA

© 2010 The Authors. Journal compilation © 2010 The Physiological Society

Downloaded from J Physiol (jp.physoc.org) at Hahneman Univ on August 6, 2010

Table 1. Properties of AMPA and NMDA EPSCs in FS interneurons in the rat prefrontal cortex

	CI (RI > 0.7) $n = 19$ (21.8%)	CP (RI < 0.7) $n = 68$ (78.2%)	*P* value
Age (days)	43.9 ± 7.29 (PD15–101)	46.4 ± 3.77 (PD15–108)	0.754
Rectification index	1.23 ± 0.06 (0.76–1.78)	0.21 ± 0.02 (0.01–0.64)	<0.0001
Resting membrane potential (mV)	−66.6 ± 3.33	−67.1 ± 1.22	0.733
Input resistance (MΩ)	210.3 ± 30.7	191.0 ± 11.6	0.240
AP threshold (mV)	−35.7 ± 2.21	−33.7 ± 1.34	0.356
AP half-width (ms)	0.56 ± 0.02	0.55 ± 0.03	0.868
Afterhyperpolarization (mV)	16.2 ± 3.46	14.4 ± 1.76	0.655
AMPA EPSC amplitude (pA)	72.4 ± 14.2	78.6 ± 7.2	0.616
AMPA EPSC decay (ms)	4.25 ± 0.53	3.92 ± 0.42	0.925
AMPA EPSC charge (pC)	0.65 ± 0.15	0.87 ± 0.10	0.421
AMPA EPSC 20–80% rise time (ms)	0.65 ± 0.06	0.67 ± 0.05	0.966
NMDA EPSC amplitude (pA)	53.4 ± 12.05	8.87 ± 1.58	<0.0001
NMDA/AMPA ratio	1.02 ± 0.12	0.19 ± 0.02	<0.0001

and NMDA receptors in the prefrontal interneurons, we recorded over 200 neurons in layers 2–5. All tested cells were initially identified under infrared differential interference contrast optics by their morphology, that is, cell bodies and multipolar dendrites. The identities of the presumptive FS interneurons were further confirmed by the following parameters: biocytin-labelled morphology, high-frequency and non-adapting firing patterns (>100 Hz, Fig. 1*A*, *B*, *D* and *E*, Table 1), and narrow half-width (mean 0.55 ± 0.04 ms) of action potentials and large fast afterhyperpolarizations (15.5 ± 0.58 mV, range 9.4–22.4 mV). These parameters are widely accepted as reliable criteria for the identification of cortical interneurons, as reported in our recent study (Wang & Gao, 2009) and in numerous previous studies (Kawaguchi, 1995; Cauli *et al.* 1997; Xiang *et al.* 1998; Gibson *et al.* 1999; Gao *et al.* 2003). Because NMDA receptors exhibited few developmental changes on the non-FS interneurons (Wang & Gao, 2009), we focused on the identified FS interneurons in this study. The remaining neurons, including pyramidal neurons and non-FS interneurons, were excluded from the dataset.

We first examined the *I–V* relationships of AMPA receptor-mediated EPSCs evoked by low-intensity stimulation of the intracortical fibres through an electrode placed ∼300 μm away from the recorded interneurons. It is known that CP-AMPARs can be blocked by endogenous intracellular polyamines (Bowie & Mayer, 1995; Kamboj *et al.* 1995; Koh *et al.* 1995). This intracellular block underlies inward rectification in the *I−V* relationship, which is presumably associated with GluR2-lacking CP-AMPARs. Although the inward rectification of CP-AMPAR channels could be lost quickly in cell-free membrane patches due to dissipation of intracellular polyamines, the loss of the rectification is prevented by adding spermine to the internal solution used to fill the patch pipette (Bowie & Mayer, 1995; Donevan & Rogawski, 1995; Koh *et al.* 1995). The AMPAR-mediated currents were recorded at −60, 0 and +60 mV, respectively, in the presence of picrotoxin (50 μM) and D-APV (50 μM) in bath solution and spermine (50 μM), a high-affinity antagonist of GluR2-lacking CP-AMPARs, included in the intracellular solution (Kamboj *et al.* 1995; Kumar *et al.* 2002). As shown in Fig. 1*C* and *F*, the *I–V* curves of the AMPA EPSCs in the individual FS interneurons were drawn, and the RIs of the EPSCs were calculated by comparing the conductance ratios of $EPSC_{+60\ mV}/EPSC_{-60\ mV}$. It is known that cells expressing appreciable levels of GluR2 receptors, which form CI-AMPARs with linear or outwardly rectifying *I–V* relationships, were usually unaffected by spermine (Toth & McBain, 1998; Kumar *et al.* 2002; Andersen *et al.* 2005). Considering the effects of the junction potential of the recording solution (about 14.9 mV), we arbitrarily set the breakup value of RI at 0.7 (Noh *et al.* 2005). Based on the *I–V* curve and the RI values (range 0.02–1.78), all recorded FS interneurons could be easily classified as either CI or CP (see Fig. 1*A–F*; Table 1). We found that most (68 of 87 or 78.1%) of the FS interneurons tested were CP cells exhibiting inwardly rectifying *I–V* curves in the presence of spermine. The RI values in most of the CP neurons were smaller than 0.5, with those in only four cells ranging from 0.51 to 0.64. In contrast, most of the CI cells had RI values ranging from 1.10 to 1.78 with the exception of four cells in which the RI values ranged from 0.76 to 0.92 (CP: $n = 68$, RI = 0.21 ± 0.02, range 0.01–0.64; CI: $n = 19$, RI = 1.23 ± 0.06, range 0.76–1.78; $P < 0.0001$; see inset between Fig. 1*C* and *F*). Despite the differences in RI ratios between CI and CP neurons, the other passive membrane properties such as resting membrane potential, input resistance, firing pattern, and half-width of action potentials appeared to be similar, without significant difference ($P > 0.05$ for all; Table 1). The other measured parameters, including amplitude, decay, charge and 20% to 80% rise time of AMPA EPSCs

© 2010 The Authors. Journal compilation © 2010 The Physiological Society

Downloaded from J Physiol (jp.physoc.org) at Hahneman Univ on August 6, 2010

recorded at −60 mV were also similar between the CI and CP interneurons, without statistical difference ($P > 0.05$ for all; Table 1). To determine whether RI was affected by the reversal potential, the AMPA EPSCs were recorded with 20 mV steps from −80 mV to +80 mV in a subset of FS interneurons (9 cells). As shown in the *I–V* relationships (Fig. 1*G* and *H*), the EPSC amplitudes were normalized to −80 mV levels, and rectification differences of EPSCs between CI and CP appeared only in the positive holding potentials. The dashed lines fitting to the EPSC amplitudes in the hyperpolarized voltage range in both CI and CP cells exhibit the deviations of the EPSC amplitudes in the depolarized voltage range from the linear fit functions. *I–V* relationships in both CI and CP interneurons exhibited similar reversal potentials without statistical difference ($P = 0.121$), but a weak correlation between RI values and reversal potential was observed (Square of correlation coefficient $R^2 = 0.389$, $P = 0.073$; Fig. 1*H*). Because the series resistance was monitored and compensated periodically, these results suggested that the contribution of voltage-clamp errors to the observed differences in rectification was minimal. In another set of experiments, we tested whether inclusion of spermine (50 μM) in the pipette affects the reversal potentials of AMPAR-mediated EPSCs. We found no difference between the FS interneurons perfused with spermine and those without spermine (reversal potential with spermine 11.9 ± 3.61 *vs.* that without spermine 13.4 ± 2.94, $n = 7$

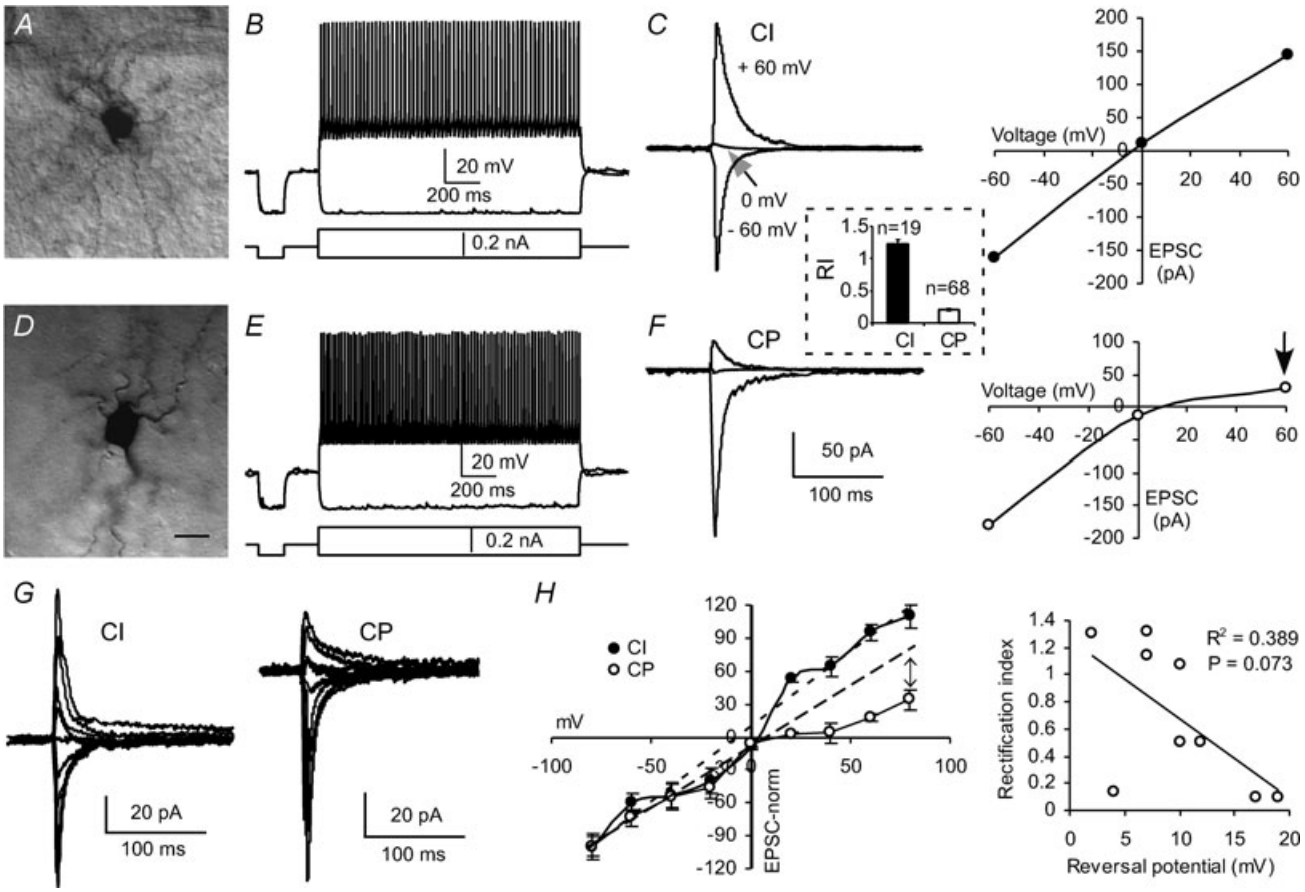

Figure 1. Two subgroups of FS interneurons in the rat medial PFC
A–C, a sample of FS interneurons exhibiting basket-like morphology (*A*), high-frequency firing (*B*), and large CI-AMPARs with high RIs (*C*, RI = 1.08). The *I–V* curve of AMPA-mediated currents in *C* was derived from the same cell used in *B*. *D–F*, a sample of FS interneurons with CP-AMPARs. Although the neurons showed similar basket-like morphology (*D*) and fired high-frequency action potentials (*E*), the AMPAR-mediated currents exhibited low RIs (arrow in *F*, RI = 0.17). Inset, the RI value in the CI interneurons ($n = 19$) was significantly higher ($P < 0.0001$) than that in the CP cells ($n = 68$). Scale bar in *D* represents 10 μm for both *A* and *D*. *G*, sample traces of evoked EPSCs at different holding potentials from −80 to +80 mV with 20 mV steps in FS interneurons containing CI- and CP-AMPARs, respectively. *H*, normalized *I–V* relationship for the EPSCs recorded as shown in *G*. The EPSCs were normalized to −80 mV levels and the data were derived from 4–5 neurons. Dashed lines: a linear fit function was applied to the EPSC amplitudes in the hyperpolarized voltage range, and the deviation of the EPSC amplitudes in the depolarized voltage range from such a fit was only obvious in the FS interneurons with CP-AMPARs (arrow). Both *I–V* relations in CI and CP interneurons exhibited similar reversal potentials without statistical difference ($P = 0.121$), but a weak correlation exists between RI values and reversal potential ($P = 0.073$).

© 2010 The Authors. Journal compilation © 2010 The Physiological Society

Downloaded from J Physiol (jp.physoc.org) at Hahneman Univ on August 6, 2010

in each group, $P = 0.748$), in agreement with a previous report (Kumar *et al.* 2002). We also did not find a clear difference in the morphologies of the FS interneurons expressing CI and CP. Most of the cells identified exhibited non-pyramidal shapes, as shown in Fig. 1*A* and *D*.

Developmental changes in CI- and CP-AMPARs in the FS interneurons

Previous studies indicated that during early postnatal development, expression of GluR2 subunits is low compared with that of GluR1, but it increases rapidly during the first postnatal week (Monyer *et al.* 1991). Consistent with these findings, synaptic GluR2-lacking AMPARs were only detected in pyramidal neurons in the neonatal neocortex (Kumar *et al.* 2002; Shin *et al.* 2007). Because the functional maturation of the PFC is postulated to be protracted and the synaptic refinement process is not completed until early adulthood (Woo *et al.* 1997; Wang *et al.* 2008), we speculated that the changes in CP-AMPARs in the PFC may be prolonged to complement the development of prefrontal functions. To test this possibility, we examined the changes in AMPARs in the FS interneurons at different developmental stages.

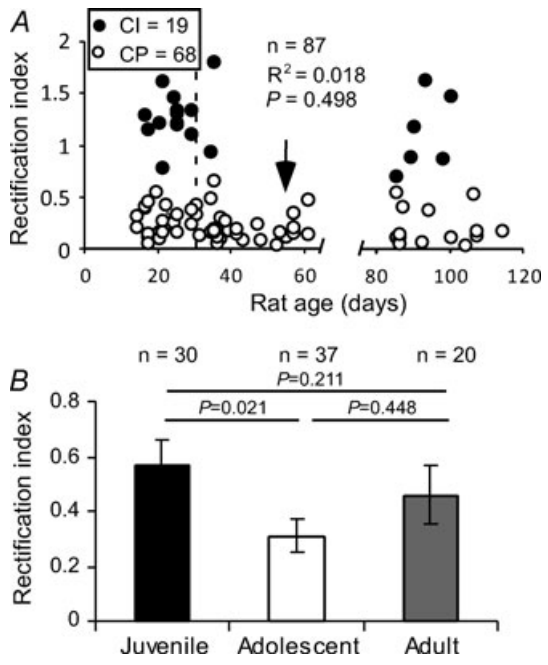

Figure 2. Developmental changes of FS interneurons containing CI- and CP-AMPARs
A, the changes of CI- and CP-AMPARs in the FS interneurons do not correlate with animal ages overall ($R^2 = 0.018$, $P = 0.498$), but a dramatic decrease in RI values was observed during the adolescent period. Most of the cells (89.2%) in this age group exhibited low RIs (arrow). *B*, FS interneurons exhibited a significant decrease in RI during the adolescent period ($P = 0.021$); the RI values were recovered in adults.

As shown in Fig. 2*A*, although the RI changes in FS neurons did not seem to be correlated with the ages of the animals ($R^2 = 0.018$, $P = 0.498$), we found significantly more cells expressing CP-AMPARs (increased by 22.5%) during the adolescent period ($\chi^2 = 5.76$, $P = 0.016$); in fact, 90% of cells in this age group exhibited low RIs (Fig. 2*A*, arrow). This trend remained until adulthood with partial recovery ($\chi^2 = 2.38$, $P = 0.123$ for juveniles *vs.* adults and $\chi^2 = 6.86$, $P = 0.087$ between adolescents and adults). Overall, the FS interneurons exhibited a significant decrease in RI values during the adolescent period (RI $= 0.57 \pm 0.09$ in juveniles *vs.* 0.31 ± 0.06 in adolescents, $P = 0.021$), and the RIs were recovered in adults ($P = 0.449$ between juveniles and adults and $P = 0.211$ between adolescents and adults). These results indicated that AMPARs exhibited significant changes during the adolescent period and that, unlike those found in the cortical pyramidal neurons (Kumar *et al.* 2002), AMPA receptors in most of the FS interneurons remained permeable to Ca^{2+} with few changes.

FS interneurons with CP-AMPA receptors express significantly fewer NMDA receptors

We recently reported that subpopulations of FS interneurons in the PFC expressed no NMDA receptors or gradually lost NMDA receptors during PFC development (Wang & Gao, 2009). We hypothesized that the NMDA receptors in the FS interneurons may be gradually replaced by CP-AMPARs to complement the need for Ca^{2+} influx during synaptic transmission. To test this possibility, we systematically examined the correlation between CP-AMPARs and NMDA receptors in the FS interneurons. The FS interneurons were identified by their firing patterns, and the AMPA EPSCs were recorded at −60, 0 and +60 mV, respectively, in the presence of picrotoxin and D-APV to examine the RI values. Then, the neurons were washed with picrotoxin and NBQX for 20 min to allow the complete recovery and isolation of NMDA EPSCs. In some cases, we recorded the NMDA EPSCs first in the presence of picrotoxin and NBQX and then, after a 20 min washout, recorded AMPA EPSCs at −60, 0 and +60 mV, respectively, in the presence of picrotoxin and D-APV. The entire process of recordings took about 35 min; stimulus intensity was kept constant during the recordings. It should be noted that although extracellular application of spermine potentiated NMDA currents in the presence of saturating concentrations of glycine (Benveniste & Mayer, 1993; Williams, 1997), no evidence suggested that intracellular spermine affected NMDA receptor channels (Williams, 1997). In addition, most of the FS interneurons expressed a significantly higher proportion of NR2A subunits (Kinney *et al.* 2006; Xi *et al.* 2009*a*,*b*), whereas spermine had no effect on the affinity of NR1A/NR2A receptors for NMDA (Williams,

© 2010 The Authors. Journal compilation © 2010 The Physiological Society

Downloaded from J Physiol (jp.physoc.org) at Hahneman Univ on August 6, 2010

1994). Indeed, under both conditions, we found that the amplitudes of either AMPA- or NMDA-EPSCs were comparable, so we pooled the data. In the FS interneurons reliably recorded for NMDA EPSCs, we found that most (18 of 19 or 94.7%) of the CI cells expressed NMDA EPSCs ranging from 7.9 to 195.6 pA, except for one cell, which expressed no NMDA current (mean 53.4 ± 12.05 pA). In contrast, the FS interneurons expressing CP-AMPARs contained either few (32/68 or 47.1%, range 0.3–36.4 pA) or no (36/68 or 52.9%) NMDA EPSCs. Accordingly, the amplitudes of NMDA EPSCs (mean 8.87 ± 1.59 pA) and of the NMDA/AMPA ratios in the FS interneurons with CP-AMPARs were significantly lower than those in the CI cells ($P < 0.0001$ for both; Fig. 3*A*–*D*). Further analysis indicated that the amplitudes of NMDA EPSCs exhibited a bimodal distribution and were clearly correlated with RI values ($n = 87$, $R^2 = 0.464$, $P < 0.0001$), with CP interneurons displaying significantly less NMDA current than CI interneurons (Fig. 3*E*). Overall, the amplitudes of NMDA EPSCs in FS interneurons were significantly lower in the adolescent period; they were very much, but not significantly, lower (due to large variability) in adult rats compared with those in juveniles (mean amplitude of NMDA currents was 31.3 ± 6.73 pA in juveniles *vs.* 10.9 ± 2.34 pA in adolescents and 14.0 ± 9.80 pA in adults, $P = 0.0037$ between juveniles and adolescents, $P = 0.071$ between juveniles and adults, and $P = 0.707$ between adolescents and adults, Fig. 3*F*). Among the CP cells, NMDA EPSCs progressively decreased, and, in the adult animals, more and more CP interneurons expressed no NMDA currents ($\chi^2 = 7.41$, $P = 0.007$, Fig. 3*G*). This result is similar to that from our previous studies, which included all (both CI and CP) FS interneurons (see Fig. 2*D* in Wang & Gao, 2009).

To further confirm the expression of NMDA receptors in FS interneurons with CI and CP AMPARs, NMDA

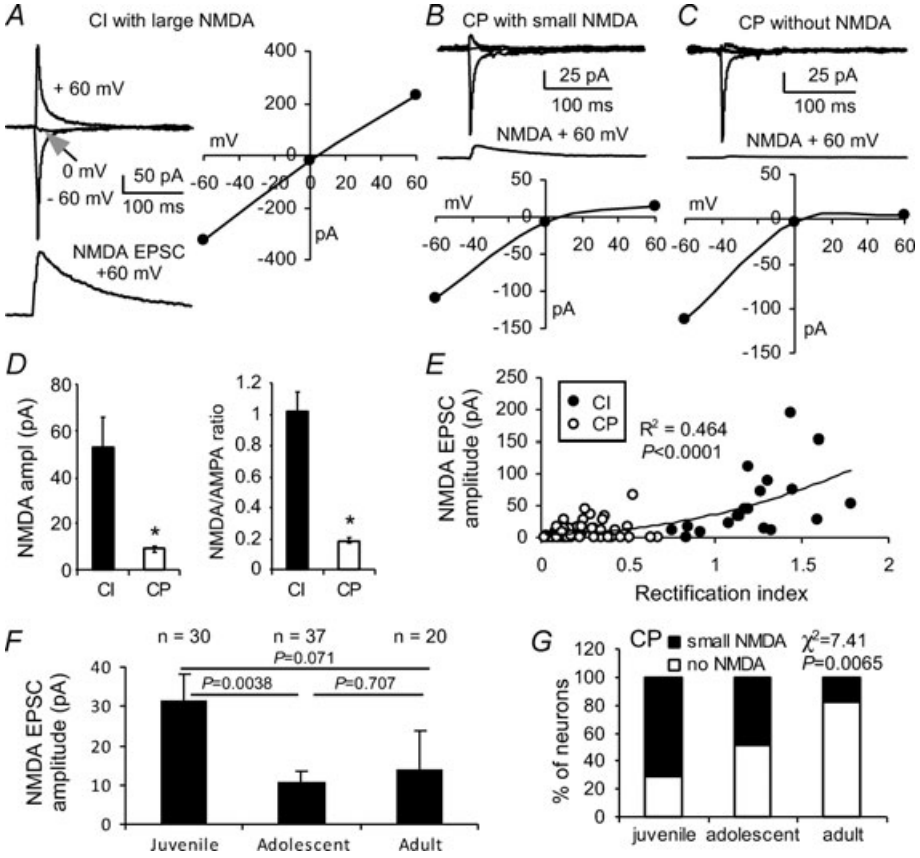

Figure 3. Correlation of CI- and CP-AMPARs with developmental changes of NMDA receptors in the FS interneurons

A–*C*, sample FS interneurons exhibiting large NMDA receptor-mediated currents in CI interneurons, but with small (*B*) or no (*C*) NMDA currents in the CP interneurons. *D* and *E*, the amplitudes of the NMDA receptor-mediated currents correlated well with the RI ($R^2 = 0.464$, $P < 0.0001$). The FS interneurons with CI-AMPARs expressed significantly more NMDA receptors compared with FS cells with CP-AMPARs, a bimodal distribution. In addition, there was a significant difference between CI and CP in the NMDA current amplitude ($^*P < 0.0001$) and NMDA/AMPA ratio ($^*P < 0.0001$). *F* and *G*, the amplitudes of NMDA EPSCs in FS interneurons were significantly decreased in adolescent and adult rats. Among these CP cells, NMDA EPSCs decreased progressively, and more and more CP interneurons expressed no NMDA currents in the adult animals.

© 2010 The Authors. Journal compilation © 2010 The Physiological Society

Downloaded from J Physiol (jp.physoc.org) at Hahneman Univ on August 6, 2010

receptor-mediated mEPSCs were recorded in two different sets of experiments. As shown in Fig. 4*A–D*, the AMPAR-mediated EPSCs in the FS interneurons were first recorded at −60, 0 and +60 mV, respectively, in the presence of picrotoxin (50 μM) and D-APV (50 μM) to determine the RI in order to identify CI and CP cells (Fig. 4*A*). The cells were then held at a membrane potential of −60 mV in a Mg^{2+}-free external solution with bath perfusion of TTX (0.5 μM) and picrotoxin (100 μM) to record the mEPSCs. Under these conditions, mEPSCs with both AMPAR- and NMDAR-mediated components were readily observed (Fig. 4*B*). The mEPSCs in the FS interneurons with CI AMPARs ($n = 6$) displayed significantly slower decay than those in the CP cells ($P < 0.05$; Fig. 4*B*). Although the amplitudes in AMPA mEPSCs in CI and CP cells were similar ($P = 0.948$), the amplitudes of

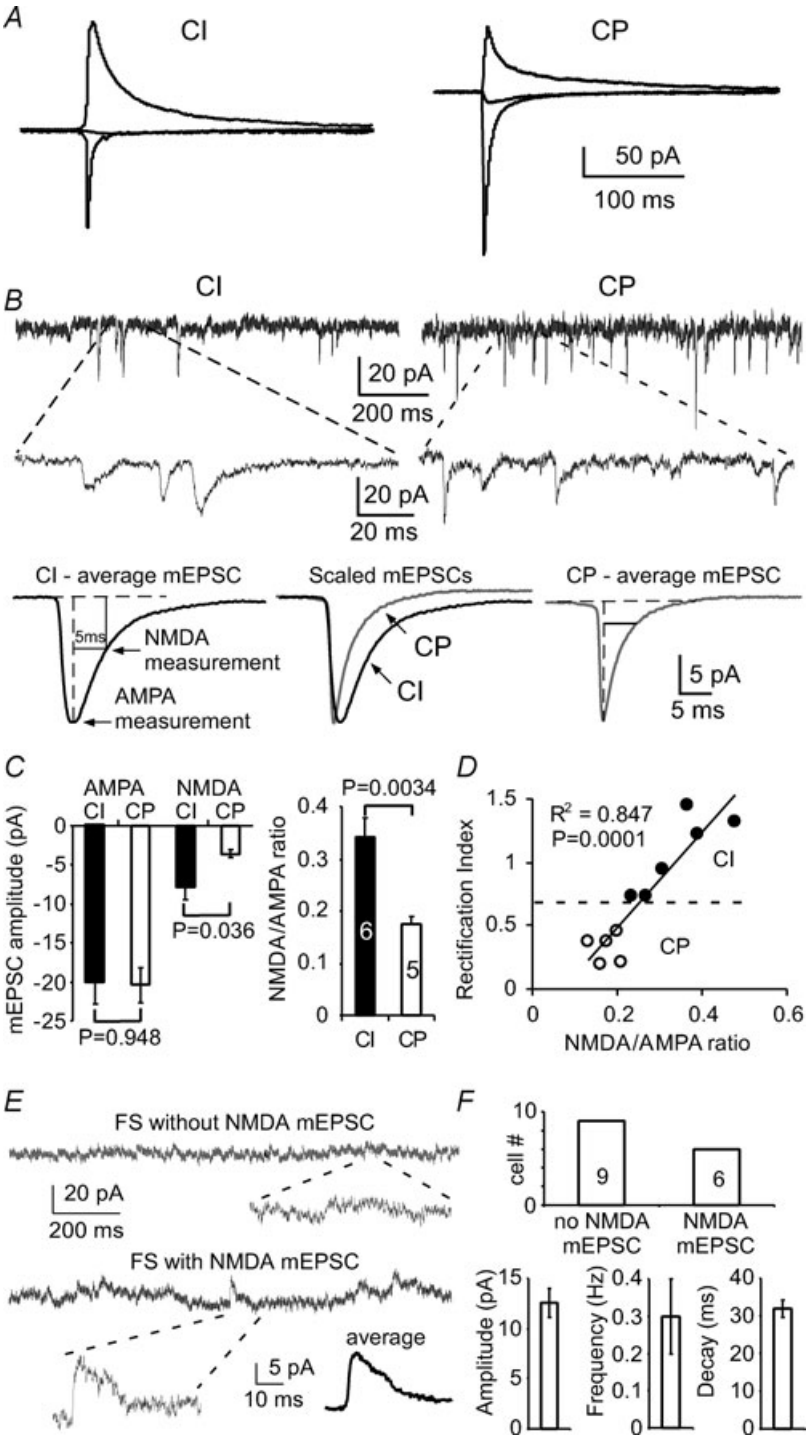

Figure 4. Distinct NMDA/AMPA ratios in FS interneurons expressing CI- and CP-AMPARs
A, AMPAR-mediated EPSCs were recorded at −60, 0 and +60 mV, respectively, in the presence of picrotoxin and D-APV. *B*, mEPSCs were recorded at −60 mV in Mg^{2+}-free external solution with bath perfusion of TTX and picrotoxin. Upper panel, example traces and expanded areas showing the mEPSCs in both CI and CP cells. Lower panel, averaged mEPSCs and measurements of both AMPA and NMDA currents. *C* and *D*, the mEPSCs in the FS interneurons with CI-AMPARs ($n = 6$) displayed significantly slower decay than those in CP cells ($P < 0.05$). The amplitudes in AMPA mEPSCs between CI and CP cells were similar ($P = 0.948$), but the amplitudes of NMDA mEPSCs were significantly different ($P = 0.036$). The FS interneurons expressing CI AMPA expressed significantly higher NMDA/AMPA ratios compared with those with CP AMPA ($P < 0.005$), and the RI values were significantly correlated with NMDA/AMPA ratios ($R^2 = 0.847$, $P = 0.0001$). *E* and *F*, in another set of experiments, the NMDA mEPSCs were recorded at +60 mV in the presence of picrotoxin, NBQX and TTX. Example traces and expanded areas in *E* showing the FS interneurons with and without NMDA mEPSCs. Among the 15 FS interneurons recorded, 9 cells exhibited no NMDA mEPSCs whereas the remaining 6 cells exhibited small NMDA currents (*F*).

© 2010 The Authors. Journal compilation © 2010 The Physiological Society

Downloaded from J Physiol (jp.physoc.org) at Hahneman Univ on August 6, 2010

NMDA mEPSCs were significantly different ($P = 0.036$; Fig. 4*C*). Therefore, the CI cells expressed significantly higher NMDA/AMPA ratios compared with those with CP AMPARs ($n = 5$, $P < 0.005$). The RI values were also significantly correlated with the NMDA/AMPA ratios ($R^2 = 0.847$, $P = 0.0001$; Fig. 4*D*). These data further confirm that FS interneurons with lower RI values express fewer NMDA receptors. To further determine whether NMDA receptors are actually lost in some FS interneurons, we conducted another set of experiments with membrane potentials held at +60 mV to record the NMDA mEPSCs in the presence of picrotoxin, NBQX and TTX. In the 15 FS interneurons recorded from rats aged PD55–63, nine cells exhibited no NMDA mEPSCs whereas the remaining six cells displayed clear NMDA currents (Fig. 4*E* and *F*). The NMDA mEPSCs were averaged at 12.6 ± 1.44 pA in amplitude, 0.30 ± 0.10 Hz in frequency, and 31.9 ± 2.47 ms in decay. These results indicate that the contribution of NMDA receptors at glutamatergic synapses onto interneurons is small or negligible, in agreement with results from a previous study of interneurons in the amygdala (Mahanty & Sah, 1998).

FS interneurons with CI- and CP-AMPA receptors exhibit different characteristics in short-term plasticity

Previous studies indicated that activity-dependent relief from polyamine block of postsynaptic CP-AMPARs in the interneurons either reduces the rate of paired-pulse depressions in a frequency-dependent manner or induces facilitation of a synaptic response that would otherwise be depressed (Rozov *et al.* 1998; Rozov & Burnashev, 1999; Toth *et al.* 2000). In addition, the firing rates of prefrontal neurons during working memory tasks in both primates (Funahashi *et al.* 1989; Miller *et al.* 1996) and rats (Fujisawa *et al.* 2008) range from 2 to 40 Hz and are averaged at 15–25 Hz. We therefore examined whether CI and CP interneurons would have different synaptic responses at the physiological firing rates observed *in vivo*. We applied 20 Hz (50 ms interstimulus interval) paired-pulse stimulation to test the short-term synaptic response in the two kinds of synapses. When the paired-pulse protocol was applied, AMPAR-mediated EPSCs at CI and CP synapses exhibited considerably different responses. We observed both paired-pulse facilitation (PPF) and depression (PPD) among the 54 FS interneurons tested (Fig. 5*A*), primarily consistent with results from previous studies (Rozov *et al.* 1998; Angulo *et al.* 1999*a*, 2003; Toth *et al.* 2000). Among these FS interneurons, however, a majority (38 of 54, 70.4%) of the cells expressed PPF with a PPR of 1.37 ± 0.05, whereas the remaining cells expressed PPD with a significantly lower PPR (16/54 or 29.6%, PPR $= 0.84 \pm 0.03$, $P < 0.0001$; Fig. 5*B*). The FS interneurons expressing PPF and PPD were again seemingly age-independent overall ($\chi^2 = 2.14$, $P = 0.342$; Fig. 5*C*), but the relative ratio of FS interneurons expressing PPF increased by 21% during the adolescent period ($\chi^2 = 9.15$, $P = 0.0025$ between juvenile and adolescent; $\chi^2 = 9.95$, $P = 0.0016$ between adolescent and adult; $\chi^2 = 0.018$, $P = 0.892$ between juvenile and adult). This change supports the significant increase of FS interneurons expressing CP-AMPARs described in Fig. 2*A* and *B*. The PPRs are slightly correlated with the age of the animal ($n = 54$, $R^2 = 0.131$, $P < 0.01$; Fig. 5*D*), with a significantly higher average PPR in adult animals compared with that in juvenile animals (1.57 ± 0.28 in adults *versus* 1.15 ± 0.05 in juveniles, $t = 2.61$, $P = 0.013$; Fig. 5*D*). Further analysis indicated that both PPF and PPD synapses were observed in CI ($n = 6$) and CP ($n = 13$) FS interneurons that were recorded in rats aged PD17–36 (Fig. 5*E*). We noted a weak negative correlation between PPR and RI ($R^2 = -0.410$, $P = 0.130$). Among these interneurons, we observed more PPD in CI neurons and more PPF in CP cells, with a significant difference between the two groups ($\chi^2 = 5.48$, $P = 0.019$). These results were consistent with those from a previous study in the hippocampus (Toth *et al.* 2000). In addition, we found that the paired-pulse responses were correlated with the distribution of NMDA receptors in both CI and CP FS interneurons. The FS interneurons expressing PPD exhibited significantly more NMDA receptors compared with FS interneurons expressing PPF, and a majority of the PPF synapses contained no NMDA receptors ($\chi^2 = 4.59$, $P = 0.032$; Fig. 5*F* and *G*).

Facilitating synapses, but not depressing synapses, are sensitive to spermine in the FS interneurons

Previous studies indicated that relief of block by intracellular polyamines was both use- and voltage-dependent (Bowie *et al.* 1998; Rozov *et al.* 1998), and CP-AMPARs were endowed with a postsynaptic mechanism for the short-term enhancement of synaptic gain (Rozov & Burnashev, 1999; Shin *et al.* 2005). We therefore examined whether polyamine analogous spermine would affect short-term plasticity at synapses expressing facilitation and depression in the FS interneurons. Paired-pulse stimulation at 20 Hz (50 ms interstimulus interval) was applied to identify synapses as either PPF or PPD in the presence or absence of spermine (50 μM) in the recording pipette. The EPSCs were recorded at −60 mV, and PPRs were calculated in the same cell at different times after the membrane break-in in whole-cell recordings. Under these conditions, we found that, when spermine was not included in the intracellular solution, the PPRs in both synapses expressing PPF and PPD were relatively stable without significant changes ($n = 4$ in each group, $P > 0.05$,

© 2010 The Authors. Journal compilation © 2010 The Physiological Society

Downloaded from J Physiol (jp.physoc.org) at Hahneman Univ on August 6, 2010

Fig. 6*A* and *B*). However, spermine significantly increased the PPRs in the FS interneurons initially expressing PPF but had little or no effect on PPRs in the FS cells expressing PPD. As shown in Fig. 6, the PPRs in the FS cells expressing PPF were gradually and significantly increased from 1.17 ± 0.06 at baseline level (mean of the EPSCs at the first 4 min after membrane break-in) to 1.67 ± 0.13 at 15 min after break-in ($n = 5$, $P = 0.020$; Fig. 6*A*). In contrast, the PPD synapses exhibited no clear change in the PPRs (0.75 ± 0.08 at 4 min *versus* 0.81 ± 0.09 at 15 min; $n = 4$, $P = 0.275$; Fig. 6*B*). These results are in agreement with those from previous studies in which polyamine-dependent facilitation occurred only in the neurons expressing CP-AMPARs, including multipolar interneurons (Rozov *et al.* 1998; Rozov & Burnashev, 1999; Toth *et al.* 2000) and immature pyramidal neurons (Shin *et al.* 2005, 2007). Furthermore, our data also support the proposition that spermine-dependent facilitation involves a postsynaptic mechanism in the FS cells expressing PPF because spermine was included in the intracellular solution (Rozov & Burnashev, 1999; Shin *et al.* 2005). Polyamines are known to modulate PKC activity, which in

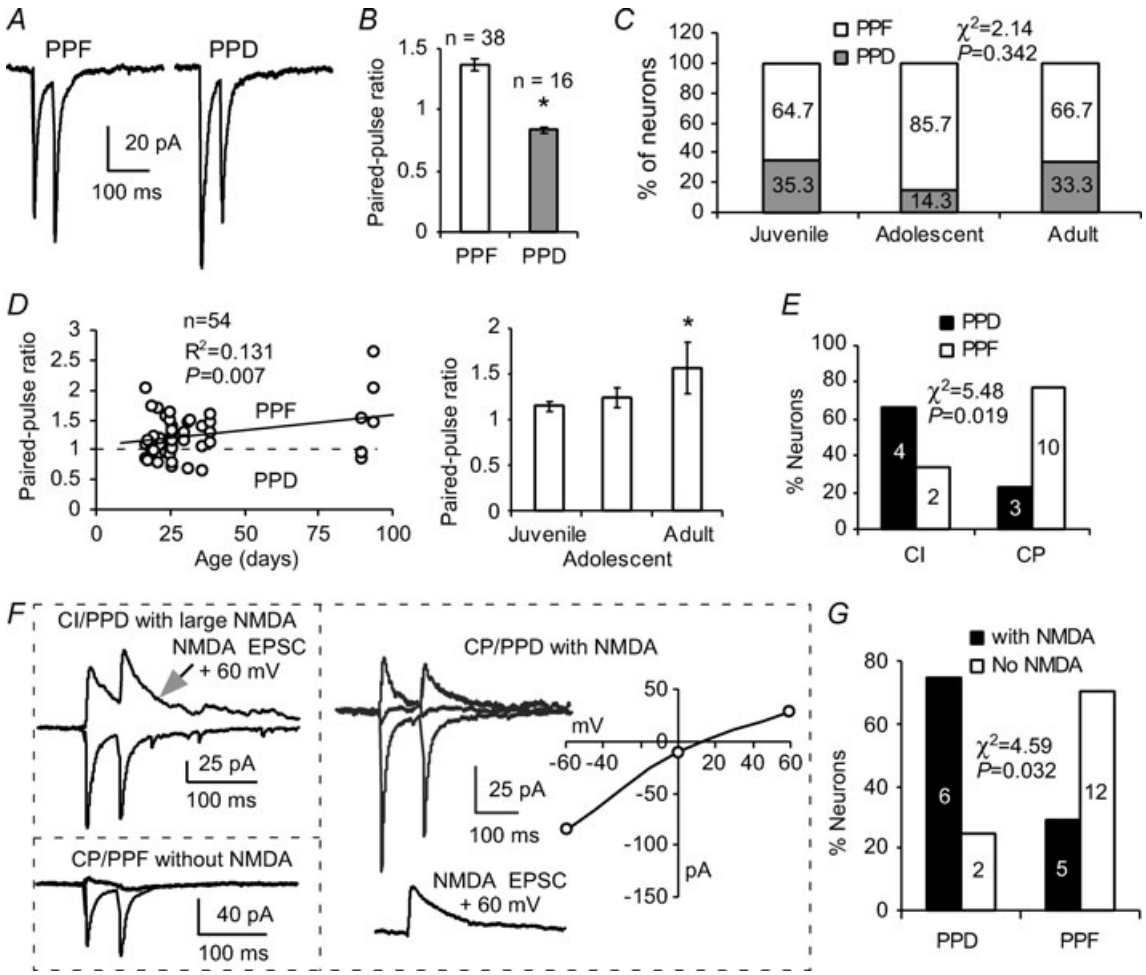

Figure 5. Correlation between PPR and RI of AMPARs, as well as NMDA receptors, in the FS interneurons
A and *B*, the AMPAR-mediated EPSCs in FS interneurons exhibited both PPF and PPD with a majority of the synapses exhibiting facilitation and about one-third showing depression (*$P < 0.0001$ in *B*). *C* and *D*, facilitating and depressing FS interneurons seemed to be age-independent overall ($P = 0.342$) despite ~20% increase of facilitating FS interneurons during the adolescent period. However, the PPR was significantly higher in adults ($P = 0.013$), and overall PPRs were correlated with postnatal ages ($n = 54$, $R^2 = 0.131$, $P = 0.007$). *E*, the PPRs were correlated with CI- and CP-AMPARs ($P = 0.019$) although both PPF and PPD synapses were seen in FS interneurons with CI- and CP-AMPARs. *F*, three samples of AMPAR- and NMDAR-mediated currents in FS interneurons exhibited PPF or PPD. Right panel, an FS interneuron with CP-AMPAR was first recorded in the presence of picrotoxin and D-APV and then after a 20 min washout, the NMDA EPSC was recorded at +60 mV in the presence of picrotoxin and NBQX. *G*, summary graph showing that PPF and PPD were closely correlated with the distribution of NMDA receptors in these interneurons, with PPF synapses containing fewer NMDA receptors than those in PPD synapses ($\chi^2 = 4.59$, $P = 0.032$).

© 2010 The Authors. Journal compilation © 2010 The Physiological Society

Downloaded from J Physiol (jp.physoc.org) at Hahneman Univ on August 6, 2010

turn enhances the phosphorylation of AMPARs and thus influences AMPAR function, particularly CP-AMPARs (Shin *et al.* 2007).

Facilitating synapses, but not depressing synapses, on FS interneurons exhibit frequency-dependent change of PPR

Previous studies indicated that synapses expressing CP-AMPARs might display short-term plasticity through postsynaptic mechanisms instead of through well-recognized presynaptic mechanisms seen in most of the synapses (Dobrunz & Stevens, 1997; Zucker & Regehr, 2002) because intracellular-loaded spermine affected the PPR (Rozov *et al.* 1998; Rozov & Burnashev, 1999; Toth *et al.* 2000; Shin *et al.* 2005). We therefore wondered whether the synapses expressing PPF and PPD displayed different frequency-dependent paired-pulse plasticity in FS interneurons in the PFC. Paired-pulse stimulation at different frequencies from 1 Hz to 100 Hz was applied in individual FS interneurons to record AMPA EPSCs at −60 mV in the presence of picrotoxin (50 μM) and D-APV (50 μM). No spermine was included in the pipette solution for Fig. 7*A–F*. Under these conditions, we found that EPSCs in facilitating FS interneurons showed a significant frequency-dependent change of the second EPSCs relative to the first EPSCs. The synapses expressed PPF at frequencies higher than 10 Hz (100 ms interval) but PPD at lower frequencies, e.g. 2 Hz, and completely recovered at 1 Hz (1000 ms interval), with a PPR of ∼1.0. For example, the PPR at 20 Hz was significantly higher than that at 2 Hz in the facilitating synapses (PPR = 1.27 ± 0.13 at 20 Hz *versus* 0.84 ± 0.03 at 2 Hz, $n = 5$, $P = 0.031$; $^*P < 0.05$ between 20 Hz and 10, 5 and 1 Hz; see Fig. 7*A–C*). In contrast to the FS interneurons expressing facilitation, the synapses exhibiting PPD continued to express depression, independent of frequency changes in the depressing FS interneuron. Both the first and second EPSCs in response to paired-pulse stimulation at different frequencies were relatively stable, without clear change in PPRs (PPR = 0.83 ± 0.07 in 20 Hz *versus* 0.79 ± 0.09 in 2 Hz, $n = 6$, $P = 0.552$; $P > 0.05$ between 20 Hz and 10, 5 and 1 Hz; Fig. 7*D–F*). These results are interesting because FS interneurons with CI-AMPARs are likely to display PPD, whereas FS interneurons with CP-AMPARs exhibit apparently more PPF. Although the direct role of CP-AMPARs in the switch of PPR in the PPF synapse remains unclear, these data indicate that FS interneurons expressing CP-AMPARs play a differential role in the neuronal integration of pyramidal neurons in the neocortex (Geiger *et al.* 1997; Angulo *et al.* 1999*b*; Sun *et al.* 2005).

Discussion

We have investigated the developmental changes in CP-AMPARs and their correlation with NMDA receptors in FS interneurons in the developing rat PFC. We found that most (∼78%) of the FS interneurons exhibit CP-AMPARs, with only one-quarter of them expressing CI-AMPARs. Although these FS interneurons displayed similar passive membrane properties, AMPAR-mediated currents at resting membrane potentials and morphologies, the FS interneurons with CP-AMPARs exhibited many distinct physiological properties, including few NMDA receptors and prominent frequency-dependent short-term facilitation. The AMPA EPSCs in FS interneurons also

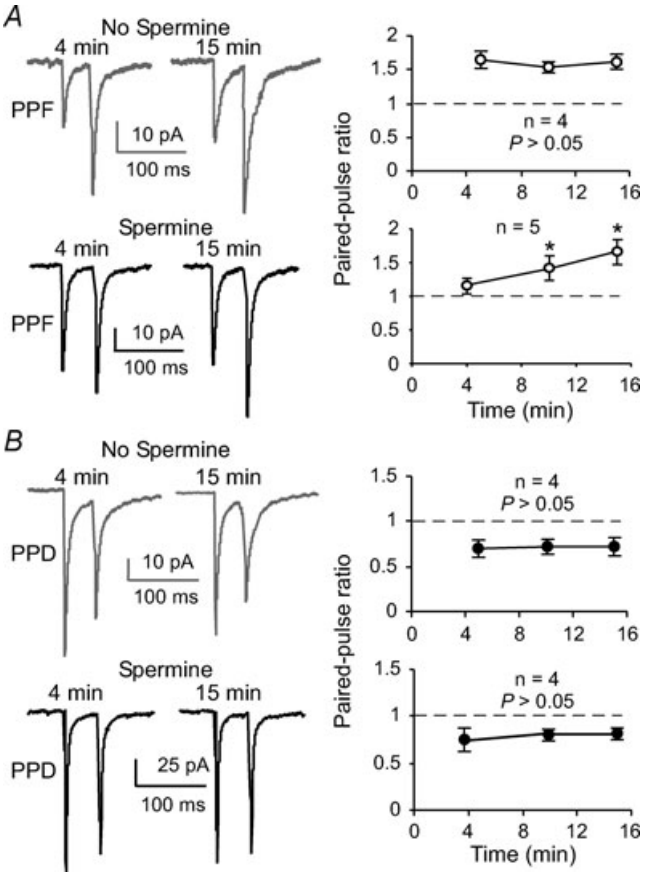

Figure 6. Spermine selectively modifies AMPA EPSCs in the facilitating FS interneurons in a time-dependent manner
A, the PPRs in synapses expressing PPF were relatively stable without significant changes when spermine was not included in the intracellular solution ($n = 4$, $P > 0.05$). Facilitating synapses in FS interneurons were, however, sensitive to spermine loaded in the recording pipette solution. The effects appeared to be time dependent. The PPRs in the FS cells expressing PPF were gradually and significantly increased ($n = 5$, $P = 0.020$; $^*P < 0.05$). *B*, in contrast, synapses expressing PPD were not affected by spermine application, and the synapses remained depressed under both conditions ($n = 4$, $P > 0.05$).

© 2010 The Authors. Journal compilation © 2010 The Physiological Society

Downloaded from J Physiol (jp.physoc.org) at Hahneman Univ on August 6, 2010

displayed a significant decrease in RI value and an increase in PPF during adolescence.

AMPARs exist as both CP and CI channels, and the presence of GluR2 subunits renders heteromeric AMPAR assemblies impermeable to Ca^{2+} (i.e. CI) (Adesnik & Nicoll, 2007). Considerable interest has centred on GluR2-lacking CP-AMPARs in the past decade because they confer novel properties on synapses and they are expressed in restricted cell populations or under certain physiological and pathological conditions (Liu & Cull-Candy, 2000; Bellone & Luscher, 2006; Clem & Barth, 2006; Cull-Candy *et al.* 2006; Plant *et al.* 2006; Isaac *et al.* 2007). The roles of such receptors in synaptic function and plasticity have been studied in hippocampal interneurons (McBain & Dingledine, 1993; Geiger *et al.* 1995; Koh *et al.* 1995; Toth & McBain, 1998, 2000; Isaac *et al.* 2007), neocortical pyramidal neurons (Kumar *et al.* 2002; Shin *et al.* 2007), and interneurons (Jonas *et al.* 1994; Rozov *et al.* 1998; Rozov & Burnashev, 1999). Although our findings supported some aspects of the results from these studies, we systematically reported for the first time the developmental changes in CP-AMPARs and their correlation with NMDA receptors in the functionally identified FS interneurons in the PFC. These findings are important because FS interneurons exhibited distinct developmental changes in NMDA receptors compared with other non-FS interneurons such as regular spiking and low-threshold spiking cells in the PFC (Wang & Gao, 2009). These data confirmed our propositions that, during prefrontal cortical development, NMDA receptors are gradually lost and that Ca^{2+} influx in FS interneurons occurs mainly through CP-AMPARs. Indeed, synaptic plasticity in FS interneurons with CP-AMPARs was usually NMDA independent (Mahanty & Sah, 1998; Laezza *et al.* 1999; Toth *et al.* 2000; Lei & McBain, 2002; Topolnik *et al.* 2005; Lamsa *et al.* 2007; Lu *et al.* 2007). In addition, we found that most of the FS interneurons with CP-AMPARs displayed comprehensible short-term facilitation compared with those expressing CI-AMPARs, which expressed more short-term depression. Because facilitating synapses in the FS interneurons are spermine-sensitive with clear voltage- (Toth *et al.* 2000; Laezza & Dingledine, 2004) and frequency-dependence (Rozov *et al.* 1998; Rozov & Burnashev, 1999; Sun *et al.* 2005), the CP and CI interneurons would have distinct roles in integrating neuronal activity in pyramidal neurons (Geiger *et al.* 1997; Angulo *et al.* 1999*a*; McBain & Fisahn, 2001; Pouille & Scanziani, 2001; Maccaferri & Dingledine, 2002; Jonas *et al.* 2004). Furthermore, unlike an apparent switch from

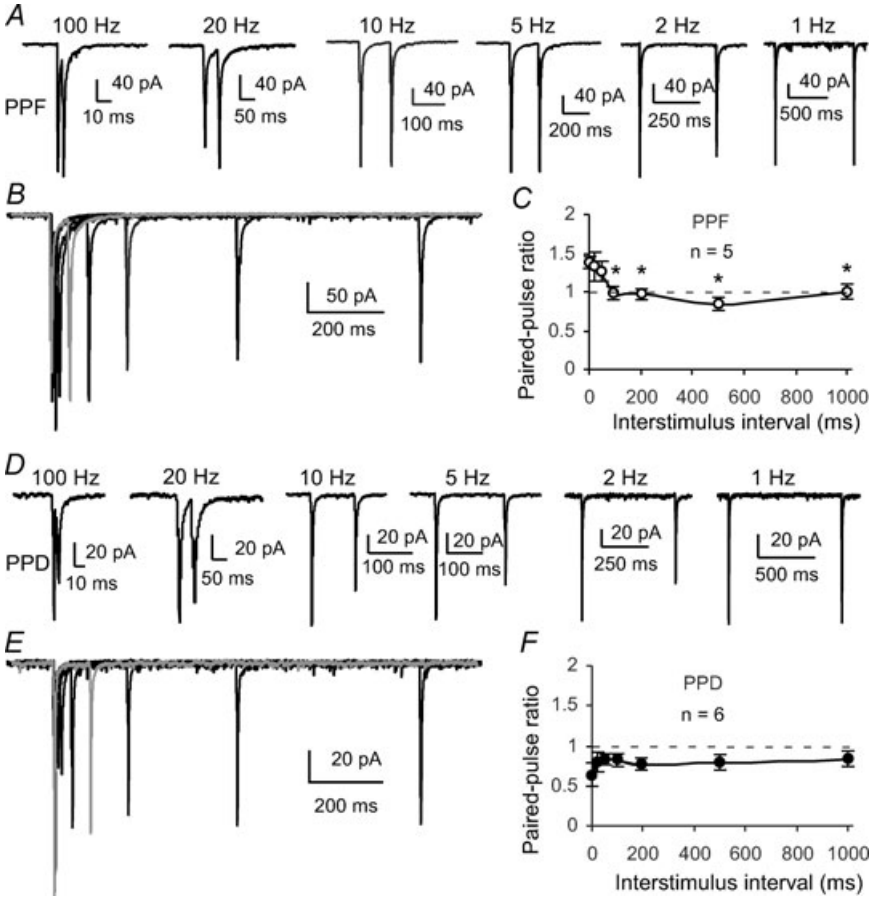

Figure 7. Frequency-dependent paired-pulse plasticity in facilitating and depressing FS interneurons
A, an example of EPSCs in a facilitating FS interneuron showing the frequency-dependent change of the second EPSC amplitudes relative to the first EPSCs. The synapse exhibited facilitation at frequencies higher than 10 Hz (100 ms interval) but expressed depression at lower frequencies such as 2 Hz and completely recovered at 1 Hz (1000 ms interval). *B*, overlap EPSC traces showing the changes of the second EPSCs relative to the first EPSCs. *C*, summary graph showing frequency-dependent change of PPR in the facilitating synapses ($n = 5$, $^*P < 0.05$ between 20 Hz and 10, 5, 2 and 1 Hz, respectively). *D*, example of a depressing FS interneuron showing the EPSCs recorded in response to paired-pulse stimulation at different frequencies. In contrast to the facilitating FS interneurons, the synapse continued to be depressed, relatively independently of frequency change. *E*, overlap traces of paired-pulse EPSCs at different frequencies in a depressing FS interneuron. *F*, summary graph showing the frequency-independent change of PPR in 6 depressing FS interneurons ($n = 6$, $P > 0.05$ between 20 Hz and 10, 5, 2 and 1 Hz, respectively).

© 2010 The Authors. Journal compilation © 2010 The Physiological Society

Downloaded from J Physiol (jp.physoc.org) at Hahneman Univ on August 6, 2010

depression in young rats (3 weeks old) to facilitation in older rats (5 weeks old) in FS interneurons in the rat motor cortex (Angulo *et al.* 1999*b*), FS interneurons in the PFC exhibited a relatively large number of PPF synapses in all age groups without significant age differences, except during the adolescent period from PD30 to PD60 (Spear, 2000; Tseng & O'Donnell, 2007). The CP-AMPAR change in adolescence is important because this period is marked by profound neuropsychological changes and by the onset of schizophrenia and other psychiatric disorders (Lewis, 1997; Spear, 2000). Indeed, a recent study reported that prefrontal cortical interneurons were more sensitive to dopaminergic modulation during adolescence (Tseng & O'Donnell, 2007). The CP-AMPARs on FS interneurons in the PFC are also clearly different from those reported in layer 5 pyramidal neurons in the rat neocortex in which GluR2-deficient CP-AMPARs were found only in rats younger than PD16 (Kumar *et al.* 2002; Shin *et al.* 2005). These results indicate that FS interneurons in the PFC undergo a developmental process in CP-AMPARs distinctly different from that of pyramidal neurons in the somatosensory cortex (Kumar *et al.* 2002; Shin *et al.* 2007) and FS interneurons in the rat motor cortex (Angulo *et al.* 1999*b*). A delayed maturation of function and receptor channels appears to be prominent in FS interneurons in the rat PFC, as shown in previous studies (Tseng & O'Donnell, 2007; Wang *et al.* 2008).

FS interneurons control the inhibitory action in pyramidal neurons (Cauli *et al.* 1997; Xiang *et al.* 1998; Gibson *et al.* 1999; Pouille & Scanziani, 2001). The dynamic properties of CP-AMPARs, evident in different forms of short- and long-term plasticity (Rozov *et al.* 1998; Rozov & Burnashev, 1999; Lei *et al.* 2002; Lei & McBain, 2004; Isaac *et al.* 2007; Lamsa *et al.* 2007), are also relevant to various neurological conditions (Liu & Zukin, 2007; Mahajan & Ziff, 2007). Changes in the expression of CP-AMPARs can alter synaptic properties or Ca^{2+}-dependent signalling cascades or can lead to injury of selectively vulnerable neurons (Tanaka *et al.* 2000; Cull-Candy *et al.* 2006). Previous studies indicate that the subunit composition of AMPARs is dynamically remodelled in a cell- and synapse-specific manner in response to neuronal activity (Liu & Cull-Candy, 2000; Ju *et al.* 2004), sensory experience (Clem & Barth, 2006; Griffiths *et al.* 2008), and neuronal insults (Tanaka *et al.* 2000; Noh *et al.* 2005; Cull-Candy *et al.* 2006). Evidence exists that, even in cells expressing high levels of GluR2, a functionally relevant population of GluR2-lacking CP-AMPARs can be surface expressed under certain conditions (Ju *et al.* 2004; Clem & Barth, 2006; Plant *et al.* 2006). Thus, understanding the regulation of GluR2-lacking CP-AMPARs is of particular importance.

The prefrontal cortex is a region of the brain involved not only in normal cognitive function such as working memory and decision making but also in many psychiatric disorders. CP-AMPARs are preferentially expressed in discrete neuronal subpopulations, and their numbers appear to be upregulated (due to decrease of GluR2) in schizophrenia (Eastwood *et al.* 1995; Beneyto & Meador-Woodruff, 2006) and other psychiatric disorders such as drug addiction (Bellone & Luscher, 2006; Conrad *et al.* 2008; Van den Oever *et al.* 2008). Because of the close correlation between Ca^{2+} permeability and inward rectification in cortical neurons (Itazawa *et al.* 1997; Liu & Zukin, 2007), these cells are extremely sensitive to detrimental stimulations that would evoke abnormal Ca^{2+} influx under certain pathological conditions. Furthermore, because of its protracted functional maturation, it is expected that the underlying synaptic refinement process in these interneurons is not completed until late adolescence and early adulthood (Woo *et al.* 1997; Tseng & O'Donnell, 2007; Wang *et al.* 2008), which would greatly increase the chance of neuronal injury under extremely stressful conditions such as drug intervention (Spear, 2000; Conrad *et al.* 2008). In summary, because of the distinct physiological properties, FS interneurons expressing CP-AMPARs play different roles in integrating neuronal information within the prefrontal cortical circuit during normal and pathophysiological activities. They also show distinct vulnerability to disruptive influences such as psychostimulants, NMDA receptor antagonists, and other agents associated with Ca^{2+} influx due to high Ca^{2+} permeability. Therefore, understanding the detailed functions of CP-AMPARs in FS interneurons will help elaborate the functional vulnerability of these cells in the pathological process of psychiatric disorders.

References

Adesnik H & Nicoll RA (2007). Conservation of glutamate receptor 2-containing AMPA receptors during long-term potentiation. *J Neurosci* **27**, 4598–4602.

Andersen TF, Vogensen SB, Jensen LS, Knapp KM & Stromgaard K (2005). Design and synthesis of labeled analogs of PhTX-56, a potent and selective AMPA receptor antagonist. *Bioorg Med Chem* **13**, 5104–5112.

Angulo MC, Lambolez B, Audinat E, Hestrin S & Rossier J (1997). Subunit composition, kinetic, and permeation properties of AMPA receptors in single neocortical nonpyramidal cells. *J Neurosci* **17**, 6685–6696.

Angulo MC, Rossier J & Audinat E (1999*a*). Postsynaptic glutamate receptors and integrative properties of fast-spiking interneurons in the rat neocortex. *J Neurophysiol* **82**, 1295–1302.

Angulo MC, Staiger JF, Rossier J & Audinat E (1999*b*). Developmental synaptic changes increase the range of integrative capabilities of an identified excitatory neocortical connection. *J Neurosci* **19**, 1566–1576.

© 2010 The Authors. Journal compilation © 2010 The Physiological Society

Downloaded from J Physiol (jp.physoc.org) at Hahneman Univ on August 6, 2010

Angulo MC, Staiger JF, Rossier J & Audinat E (2003). Distinct local circuits between neocortical pyramidal cells and fast-spiking interneurons in young adult rats. *J Neurophysiol* **89**, 943–953.

Bellone C & Luscher C (2006). Cocaine triggered AMPA receptor redistribution is reversed *in vivo* by mGluR-dependent long-term depression. *Nat Neurosci* **9**, 636–641.

Beneyto M & Meador-Woodruff JH (2006). Lamina-specific abnormalities of AMPA receptor trafficking and signaling molecule transcripts in the prefrontal cortex in schizophrenia. *Synapse* **60**, 585–598.

Benveniste M & Mayer ML (1993). Multiple effects of spermine on *N*-methyl-D-aspartic acid receptor responses of rat cultured hippocampal neurones. *J Physiol* **464**, 131–163.

Blatow M, Caputi A & Monyer H (2005). Molecular diversity of neocortical GABAergic interneurones. *J Physiol* **562**, 99–105.

Bowie D, Lange GD & Mayer ML (1998). Activity-dependent modulation of glutamate receptors by polyamines. *J Neurosci* **18**, 8175–8185.

Bowie D & Mayer ML (1995). Inward rectification of both AMPA and kainate subtype glutamate receptors generated by polyamine-mediated ion channel block. *Neuron* **15**, 453–462.

Cauli B, Audinat E, Lambolez B, Angulo MC, Ropert N, Tsuzuki K, Hestrin S & Rossier J (1997). Molecular and physiological diversity of cortical nonpyramidal cells. *J Neurosci* **17**, 3894–3906.

Clem RL & Barth A (2006). Pathway-specific trafficking of native AMPARs by in vivo experience. *Neuron* **49**, 663–670.

Conrad KL, Tseng KY, Uejima JL, Reimers JM, Heng L-J, Shaham Y, Marinelli M & Wolf ME (2008). Formation of accumbens GluR2-lacking AMPA receptors mediates incubation of cocaine craving. *Nature* **454**, 118–121.

Cull-Candy S, Kelly L & Farrant M (2006). Regulation of Ca^{2+}-permeable AMPA receptors: synaptic plasticity and beyond. *Curr Opin Neurobiol* **16**, 288–297.

Dobrunz LE & Stevens CF (1997). Heterogeneity of release probability, facilitation, and depletion at central synapses. *Neuron* **18**, 995–1008.

Donevan SD & Rogawski MA (1995). Intracellular polyamines mediate inward rectification of Ca^{2+}-permeable α-amino-3-hydroxy-5-methyl-4-isoxazolepropionic acid receptors. *Proc Natl Acad Sci U S A* **92**, 9298–9302.

Drummond GB (2009). Reporting ethical matters in *The Journal of Physiology*: standards and advice. *J Physiol* **587**, 713–719.

Eastwood SL, McDonald B, Burnet PW, Beckwith JP, Kerwin RW & Harrison PJ (1995). Decreased expression of mRNAs encoding non-NMDA glutamate receptors GluR1 and GluR2 in medial temporal lobe neurons in schizophrenia. *Brain Res Mol Brain Res* **29**, 211–223.

Fujisawa S, Amarasingham A, Harrison MT & Buzsaki G (2008). Behavior-dependent short-term assembly dynamics in the medial prefrontal cortex. *Nat Neurosci* **11**, 823–833.

Funahashi S, Bruce CJ & Goldman-Rakic PS (1989). Mnemonic coding of visual space in the monkey's dorsolateral prefrontal cortex. *J Neurophysiol* **61**, 331–349.

Gao WJ (2007). Acute clozapine suppresses synchronized pyramidal synaptic network activity by increasing inhibition in the ferret prefrontal cortex. *J Neurophysiol* **97**, 1196–1208.

Gao WJ & Goldman-Rakic PS (2003). Selective modulation of excitatory and inhibitory microcircuits by dopamine. *Proc Natl Acad Sci U S A* **100**, 2836–2841.

Gao WJ, Wang Y & Goldman-Rakic PS (2003). Dopamine modulation of perisomatic and peridendritic inhibition in prefrontal cortex. *J Neurosci* **23**, 1622–1630.

Geiger JR, Lubke J, Roth A, Frotscher M & Jonas P (1997). Submillisecond AMPA receptor-mediated signaling at a principal neuron–interneuron synapse. *Neuron* **18**, 1009–1023.

Geiger JR, Melcher T, Koh DS, Sakmann B, Seeburg PH, Jonas P & Monyer H (1995). Relative abundance of subunit mRNAs determines gating and Ca^{2+} permeability of AMPA receptors in principal neurons and interneurons in rat CNS. *Neuron* **15**, 193–204.

Gibson JR, Beierlein M & Connors BW (1999). Two networks of electrically coupled inhibitory neurons in neocortex. *Nature* **402**, 75–79.

Goldberg JH, Yuste R & Tamas G (2003). Ca^{2+} imaging of mouse neocortical interneuron dendrites: contribution of Ca^{2+}-permeable AMPA and NMDA receptors to subthreshold Ca^{2+} dynamics. *J Physiol* **551**, 67–78.

Griffiths S, Scott H, Glover C, Bienemann A, Ghorbel MT, Uney J, Brown MW, Warburton EC & Bashir ZI (2008). Expression of long-term depression underlies visual recognition memory. *Neuron* **58**, 186–194.

Hestrin S (1993). Different glutamate receptor channels mediate fast excitatory synaptic currents in inhibitory and excitatory cortical neurons. *Neuron* **11**, 1083–1091.

Hollmann M & Heinemann S (1994). Cloned glutamate receptors. *Annu Rev Neurosci* **17**, 31–108.

Isaac JT, Ashby M & McBain CJ (2007). The role of the GluR2 subunit in AMPA receptor function and synaptic plasticity. *Neuron* **54**, 859–871.

Itazawa SI, Isa T & Ozawa S (1997). Inwardly rectifying and Ca^{2+}-permeable AMPA-type glutamate receptor channels in rat neocortical neurons. *J Neurophysiol* **78**, 2592–2601.

Jonas P, Bischofberger J, Fricker D & Miles R (2004). Interneuron Diversity series: Fast in, fast out – temporal and spatial signal processing in hippocampal interneurons. *Trends Neurosci* **27**, 30–40.

Jonas P & Burnashev N (1995). Molecular mechanisms controlling calcium entry through AMPA-type glutamate receptor channels. *Neuron* **15**, 987–990.

Jonas P, Racca C, Sakmann B, Seeburg PH & Monyer H (1994). Differences in Ca^{2+} permeability of AMPA-type glutamate receptor channels in neocortical neurons caused by differential GluR-B subunit expression. *Neuron* **12**, 1281–1289.

Ju W, Morishita W, Tsui J, Gaietta G, Deerinck T, Adams S, Garner C, Tsien R, Ellisman M & Malenka R (2004). Activity-dependent regulation of dendritic synthesis and trafficking of AMPA receptors. *Nat Neurosci* **7**, 244–253.

Kamboj SK, Swanson GT & Cull-Candy SG (1995). Intracellular spermine confers rectification on rat calcium-permeable AMPA and kainate receptors. *J Physiol* **486**, 297–303.

Kawaguchi Y (1995). Physiological subgroups of nonpyramidal cells with specific morphological characteristics in layer II/III of rat frontal cortex. *J Neurosci* **15**, 2638–2655.

© 2010 The Authors. Journal compilation © 2010 The Physiological Society

Downloaded from J Physiol (jp.physoc.org) at Hahneman Univ on August 6, 2010

Kinney JW, Davis CN, Tabarean I, Conti B, Bartfai T & Behrens MM (2006). A specific role for NR2A-containing NMDA receptors in the maintenance of parvalbumin and GAD67 immunoreactivity in cultured interneurons. *J Neurosci* **26**, 1604–1615.

Koh DS, Burnashev N & Jonas P (1995). Block of native Ca^{2+}-permeable AMPA receptors in rat brain by intracellular polyamines generates double rectification. *J Physiol* **486**, 305–312.

Kumar SS, Bacci A, Kharazia V & Huguenard JR (2002). A developmental switch of AMPA receptor subunits in neocortical pyramidal neurons. *J Neurosci* **22**, 3005–3015.

Laezza F & Dingledine R (2004). Voltage-controlled plasticity at GluR2-deficient synapses onto hippocampal interneurons. *J Neurophysiol* **92**, 3575–3581.

Laezza F, Doherty JJ & Dingledine R (1999). Long-term depression in hippocampal interneurons: joint requirement for pre- and postsynaptic events. *Science* **285**, 1411–1414.

Lamsa KP, Heeroma JH, Somogyi P, Rusakov DA & Kullmann DM (2007). Anti-Hebbian long-term potentiation in the hippocampal feedback inhibitory circuit. *Science* **315**, 1262–1266.

Lei G, Xue S, Chery N, Liu Q, Xu J, Kwan CL, Fu YP, Lu YM, Liu M, Harder KW & Yu XM (2002). Gain control of *N*-methyl-D-aspartate receptor activity by receptor-like protein tyrosine phosphatase α. *EMBO J* **21**, 2977–2989.

Lei S & McBain CJ (2002). Distinct NMDA receptors provide differential modes of transmission at mossy fiber–interneuron synapses. *Neuron* **33**, 921–933.

Lei S & McBain CJ (2004). Two loci of expression for long-term depression at hippocampal mossy fiber–interneuron synapses. *J Neurosci* **24**, 2112–2121.

Lewis DA (1997). Development of the prefrontal cortex during adolescence: insights into vulnerable neural circuits in schizophrenia. *Neuropsychopharmacol* **16**, 385–398.

Liu B, Liao M, Mielke JG, Ning K, Chen Y, Li L, El-Hayek YH, Gomez E, Zukin RS, Fehlings MG & Wan Q (2006). Ischemic insults direct glutamate receptor subunit 2-lacking AMPA receptors to synaptic sites. *J Neurosci* **26**, 5309–5319.

Liu SJ & Zukin RS (2007). Ca^{2+}-permeable AMPA receptors in synaptic plasticity and neuronal death. *Trends Neurosci* **30**, 126–134.

Liu SQ & Cull-Candy SG (2000). Synaptic activity at calcium-permeable AMPA receptors induces a switch in receptor subtype. *Nature* **405**, 454–458.

Lu J-t, Li C-y, Zhao J-P, Poo M-m & Zhang X-h. (2007). Spike-timing-dependent plasticity of neocortical excitatory synapses on inhibitory interneurons depends on target cell type. *J Neurosci* **27**, 9711–9720.

McBain CJ & Dingledine R (1993). Heterogeneity of synaptic glutamate receptors on CA3 stratum radiatum interneurones of rat hippocampus. *J Physiol* **462**, 373–392.

McBain CJ & Fisahn A (2001). Interneurons unbound. *Nat Rev Neurosci* **2**, 11–23.

Maccaferri G & Dingledine R (2002). Control of feedforward dendritic inhibition by NMDA receptor-dependent spike timing in hippocampal interneurons. *J Neurosci* **22**, 5462–5472.

Mahajan SS & Ziff EB (2007). Novel toxicity of the unedited GluR2 AMPA receptor subunit dependent on surface trafficking and increased Ca^{2+}-permeability. *Mol Cell Neurosci* **35**, 470–481.

Mahanty N & Sah P (1998). Calcium-permeable AMPA receptors mediate long term potentiation in interneurons of the amygdala. *Nature* **394**, 683–687.

Miller EK, Erickson CA & Desimone R (1996). Neural mechanisms of visual working memory in prefrontal cortex of the macaque. *J Neurosci* **16**, 5154–5167.

Monyer H, Seeburg PH & Wisden W (1991). Glutamate-operated channels: developmentally early and mature forms arise by alternative splicing. *Neuron* **6**, 799–810.

Myme CI, Sugino K, Turrigiano GG & Nelson SB (2003). The NMDA-to-AMPA ratio at synapses onto layer 2/3 pyramidal neurons is conserved across prefrontal and visual cortices. *J Neurophysiol* **90**, 771–779.

Noh KM, Yokota H, Mashiko T, Castillo PE, Zukin RS & Bennett MV (2005). Blockade of calcium-permeable AMPA receptors protects hippocampal neurons against global ischemia-induced death. *Proc Natl Acad Sci U S A* **102**, 12230–12235.

Plant K, Pelkey KA, Bortolotto ZA, Morita D, Terashima A, McBain CJ, Collingridge GL & Isaac JTR (2006). Transient incorporation of native GluR2-lacking AMPA receptors during hippocampal long-term potentiation. *Nat Neurosci* **9**, 602–604.

Pouille F & Scanziani M (2001). Enforcement of temporal fidelity in pyramidal cells by somatic feed-forward inhibition. *Science* **293**, 1159–1163.

Rozov A & Burnashev N (1999). Polyamine-dependent facilitation of postsynaptic AMPA receptors counteracts paired-pulse depression. *Nature* **401**, 594–598.

Rozov A, Zilberter Y, Wollmuth LP & Burnashev N (1998). Facilitation of currents through rat Ca^{2+}-permeable AMPA receptor channels by activity-dependent relief from polyamine block. *J Physiol* **511**, 361–377.

Shin J, Shen F & Huguenard J (2007). PKC and polyamine modulation of GluR2-deficient AMPA receptors in immature neocortical pyramidal neurons of the rat. *J Physiol* **581**, 679–691.

Shin J, Shen F & Huguenard JR (2005). Polyamines modulate AMPA receptor-dependent synaptic responses in immature layer V pyramidal neurons. *J Neurophysiol* **93**, 2634–2643.

Spear LP (2000). The adolescent brain and age-related behavioral manifestations. *Neurosci Biobehav Rev* **24**, 417–463.

Sun HY, Lyons SA & Dobrunz LE (2005). Mechanisms of target-cell specific short-term plasticity at Schaffer collateral synapses onto interneurones *versus* pyramidal cells in juvenile rats. *J Physiol* **568**, 815–840.

Tanaka H, Grooms SY, Bennett MV & Zukin RS (2000). The AMPAR subunit GluR2: still front and center-stage. *Brain Res* **886**, 190–207.

Topolnik L, Congar P & Lacaille JC (2005). Differential regulation of metabotropic glutamate receptor- and AMPA receptor-mediated dendritic Ca^{2+} signals by presynaptic and postsynaptic activity in hippocampal interneurons. *J Neurosci* **25**, 990–1001.

© 2010 The Authors. Journal compilation © 2010 The Physiological Society

Downloaded from J Physiol (jp.physoc.org) at Hahneman Univ on August 6, 2010

Toth K & McBain CJ (1998). Afferent-specific innervation of two distinct AMPA receptor subtypes on single hippocampal interneurons. *Nat Neurosci* **1**, 572–578.

Toth K & McBain CJ (2000). Target-specific expression of pre- and postsynaptic mechanisms. *J Physiol* **525**, 41–51.

Toth K, Suares G, Lawrence JJ, Philips-Tansey E & McBain CJ (2000). Differential mechanisms of transmission at three types of mossy fiber synapse. *J Neurosci* **20**, 8279–8289.

Tseng KY & O'Donnell P (2007). Dopamine modulation of prefrontal cortical interneurons changes during adolescence. *Cereb Cortex* **17**, 1235–1240.

Van Den Oever MC, Goriounova NA, Wan Li K, Van Der Schors RC, Binnekade R, Schoffelmeer ANM, Mansvelder HD, Smit AB, Spijker S & De Vries TJ (2008). Prefrontal cortex AMPA receptor plasticity is crucial for cue-induced relapse to heroin-seeking. *Nat Neurosci* **11**, 1053–1058.

Wang H, Stradtman GG 3rd, Wang XJ & Gao WJ (2008). A specialized NMDA receptor function in layer 5 recurrent microcircuitry of the adult rat prefrontal cortex. *Proc Natl Acad Sci U S A* **105**, 16791–16796.

Wang HX & Gao WJ (2009). Cell type-specific development of NMDA receptors in the interneurons of rat prefrontal cortex. *Neuropsychopharmacology* **34**, 2028–2040.

Williams K (1994). Mechanisms influencing stimulatory effects of spermine at recombinant N-methyl-D-aspartate receptors. *Mol Pharmacol* **46**, 161–168.

Williams K (1997). Interactions of polyamines with ion channels. *Biochem J* **325**, 289–297.

Woo TU, Pucak ML, Kye CH, Matus CV & Lewis DA (1997). Peripubertal refinement of the intrinsic and associational circuitry in monkey prefrontal cortex. *Neuroscience* **80**, 1149–1158.

Xi D, Keeler B, Zhang W, Houle JD & Gao WJ (2009*a*). NMDA receptor subunit expression in GABAergic interneurons in the prefrontal cortex: application of laser micro dissection technique. *J Neurosci Methods* **176**, 172–181.

Xi D, Zhang W, Wang HX, Stradtman GG & Gao WJ (2009*b*). Dizocilpine (MK-801) induces distinct changes of *N*-methyl-D-aspartic acid receptor subunits in parvalbumin-containing interneurons in young adult rat prefrontal cortex. *Int J Neuropsychopharmacol* **12**, 1395–1408.

Xiang Z, Huguenard JR & Prince DA (1998). Cholinergic switching within neocortical inhibitory networks. *Science* **281**, 985–988.

Zucker RS & Regehr WG (2002). Short-term synaptic plasticity. *Annu Rev Physiol* **64**, 355–405.

Author contributions

W.-J.G. conceived the study, supervised the project, and wrote the manuscript. H.-X.W. carried out the experiments and data analysis. H.-X.W. also contributed to the manuscript preparation.

Acknowledgements

We thank Dr Jeremy Cohen for comments on the manuscript and Ms Pamela Fried at DUCOM Academic Publishing Services for editorial work. This study was supported by a grant from Drexel University College of Medicine, NARSAD young investigator awards, and the National Institutes of Health (R21MH232307 and R01MH232395) to W.-J. Gao. The NIH had no role in the study design; in the collection, analysis, and interpretation of the data; in the writing of the report; or in the decision to submit the paper for publication. The authors have no financial conflict of interest to disclose.

© 2010 The Authors. Journal compilation © 2010 The Physiological Society

Downloaded from J Physiol (jp.physoc.org) at Hahneman Univ on August 6, 2010